NUMERICAL EXPERIMENTS WITH HIGH-ORDER ADVECTIVE EQUATIONS

by

Dean Russell Morford

UNITED STATES
NAVAL POSTGRADUATE SCHOOL

THESIS

NUMERICAL EXPERIMENTS WITH

HIGH-ORDER ADVECTIVE EQUATIONS

by

Dean Russell Morford

December 1968

NUMERICAL EXPERIMENTS WITH

HIGH-ORDER ADVECTIVE EQUATIONS

by

Dean Russell Morford
Commander, United States Navy
B.S., North Dakota State University, 1953

Submitted in partial fulfillment of the
requirements for the degree of

MASTER OF SCIENCE IN METEOROLOGY

from the

NAVAL POSTGRADUATE SCHOOL
December 1968

ABSTRACT

Second-order and fourth-order two-dimensional advective equations developed by W. P. Crowley were examined to determine their applicability to atmospheric models.

One second-order and two fourth-order forms were evaluated from their performances on a simple pattern advected by a linear, divergent velocity field. The same equations were substituted for the advection term of a simple barotropic forecast model to determine their performances on more general non-linear conditions.

All forms of the equations remained stable in time and demonstrated the phase and amplitude characteristics predicted by Crowley. The fourth-order "advection" form gave best results.

When substituted in the barotropic model, the fourth-order forms lead to improved trough and low-center movements, but RMSE was slightly larger than that resulting from second-order forms. The better RMSE of the lower order forms apparently resulted from their diffusive charateristics.

TABLE OF CONTENTS

LIST OF TABLES

LIST OF ILLUSTRATIONS

TABLE OF SYMBOLS AND ABBREVIATIONS

RMSE	Root mean square error
ϕ	Any conservative parameter
$\vec{V}$	Horizontal wind velocity
∇	Horizontal del operator
u	x -component of wind
v	y -component of wind
J	Jacobian operator
Ψ	Stream function
t	Time
η	Absolute vorticity
F	Flux
I	Identity matrix
A	Linear difference operator in x-direction
B	Linear difference operator in y-direction
k_x	Divergence in x-direction
k_y	Divergence in y-direction
R	Number of grid intervals from a given point
R_c	Number of grid intervals from grid center
d	Standard distance between grid-points
S	Number of time steps
M	Velocity factor
N	Divergence factor
μ	Constant
f	Coriolis parameter

Z	Height
F_a	Advective forcing function
g	Acceleration of gravity
FNWC	Fleet Numerical Weather Central, Monterey, California
C4	Fourth-order conservation method of advection
A4	Fourth-order advection method
A2	Second-order advection method
J1	Common Jacobian method
MB	Millibar
m.	Meter
sec.	Second
σ_η^2	Variance of absolute vorticity
m	Map factor
$\overline{(\ )}$	Average Value
n	Time dimension superscript
i	x-coordinate subscript
j	y-coordinate subscript

ACKNOWLEDGMENTS

My appreciation is extended to Professor G. J. Haltiner for his patient guidance and to Captain P. M. Wolff, USN, Commanding Officer, Fleet Numerical Weather Central, for the assistance provided by his staff.

CHAPTER I

INTRODUCTION

The hydrodyamical equations governing fluid motion usually contain a non-linear advective or transport term which often plays an important role with respect to the temporal changes of the pertinent parameters. It is, therefore, desirable to approximate the advective term accurately when a numerical solution of the equations is sought.

In order to investigate the accuracy of various finite-difference representations of the transport term, it will be assumed that some parameter, ϕ, is conserved in a two-dimensional flow field. This assumption may be expressed in Eulerian form as

$$\frac{\partial \phi}{\partial t} = - \vec{V} \cdot \nabla \phi, \tag{1.1}$$

where $\vec{V}$ is the horizontal velocity and ∇ is the two-dimensional del operator.

When written in scalar form, eq. 1.1 becomes

$$\frac{\partial \phi}{\partial t} = - \left[u \frac{\partial \phi}{\partial x} + v \frac{\partial \phi}{\partial y} \right], \tag{1.2}$$

where u and v are the x and y components, respectively, of the vector velocity. If the flow is non-divergent, eq. 1.2 may be expressed as

$$\frac{\partial \phi}{\partial t} = - J(\Psi, \phi), \tag{1.3}$$

where Ψ is the stream function and J is the well-known Jacobian operator.

An expression equivalent to eq. 1.2 is

$$\frac{\partial \phi}{\partial t} = - \left[\frac{\partial (\phi u)}{\partial x} + \frac{\partial (\phi v)}{\partial y} - \phi \left(\frac{\partial u}{\partial x} + \frac{\partial v}{\partial y} \right) \right]. \tag{1.4}$$

Although the analytical solution to eq. 1.4 is identical to that of eq. 1.2, the latter form leads to a different finite-difference expression possessing certain advantages which are discussed in Chapter II.

For convenience, the advective equation as expressed by eq. 1.2 will be called the "advection" form; equation 1.4 will be referred to as the "conservation" form.

Although the analytical solution of a differential equation is exact, the finite-difference representation is only an approximation. When modern digital computers are utilized, the accuracy of the approximation is principally dependent on (1) truncation error, and (2) computational stability. Truncation error may be reduced (but never eliminated) by retaining high-order terms and by reducing the size of the grid-mesh. Elimination of instability error is more difficult because computational stability is dependent on the physical properties of the fluid as well as on the specific form of the finite-difference equation.

Many finite-difference techniques have resulted from attempts to control instability while reducing truncation error. The purpose of this study was to evaluate by numerical experimentation the applicability to the atmosphere of high-order, two-dimensional advective techniques proposed by Crowley [1].

Examples of practical problems which require accurate advective techniques are (1) radioactive debris tracking, (2) air and water pollution studies, (3) estimation of movement and concentration of potentially lethal gases, and (4) numerical weather prediction. Numerical models which provide solutions to these problems often require a high degree of accuracy throughout long periods of time.

For example, radioactive debris projected into the stratosphere may travel around the earth several times before the combined effects of turbulent diffusion, velocity divergence and deformation, and fall-out reduce the concentration of the radioactive substance to an insignificant level.

A good advection scheme, therefore, must exhibit not only small errors in each time step, but also small cumulative errors after many steps. To determine the extent to which Crowley's equations satisfy this requirement, the initial experiment was designed to evaluate the performance of the techniques, given a known configuration of a conservative quantity and a known velocity field. From observations of the position, shape, and magnitude of the quantity after many hours of advection, statistics on effective phase speed, conservation of intensity and shape, and computational stability were obtained.

Since diagnostic and prognostic models of the atmosphere must approximate real conditions in a satisfactory manner, the advective terms employed must demonstrate stability and accuracy under non-linear conditions. The characteristics of Crowley's equations, given non-linear conditions, were evaluated by comparing the results obtained from a simple barotropic forecast model in which appropriate forms of the various advective equations were utilized.

CHAPTER II

THE ADVECTIVE EQUATIONS

The alternate forms of the advective equation will be developed in this chapter. Both result in a forward time step based upon centered space differences. Since the resulting finite-difference equations will be used eventually in the barotropic model, absolute vorticity, η, will be substituted for ϕ in eqs. 1.1 - 1.4.

The following is an explanation of the notation used to indicate time and space differences:

1. Superscript n: denotes the current hour.
2. Subscript i: denotes the x-coordinate of the grid point, $x = i\Delta x$.
3. Subscript j: denotes the y-coordinate of the grid point, $y = j\Delta y$.

The development of equations 1.2 and 1.4 follows closely that of Crowley with minor differences in notation.

THE ADVECTION FORM

A Taylor series expansion in time of equation 1.2 in one dimension results in

$$\eta_i^{n+1} = \eta_i^n + \Delta t \left.\frac{\partial \eta}{\partial t}\right|_i^n + \frac{(\Delta t)^2}{2} \left.\frac{\partial^2 \eta}{\partial t^2}\right|_i^n + O(\Delta t^3). \tag{2.1}$$

From equation 1.2,

$$\frac{\partial \eta}{\partial t} = - u \frac{\partial \eta}{\partial x} . \tag{2.2}$$

Differentiating the above equation with respect to time gives

$$\frac{\partial^2 \eta}{\partial t^2} = - \left[\frac{\partial u}{\partial t} \frac{\partial \eta}{\partial x} + u \frac{\partial}{\partial t} \left(\frac{\partial \eta}{\partial x}\right)\right].$$

If the order of differentiation is changed in the last term, and substitution is made from eq. 2.2, the result is

$$\frac{\partial^2 \eta}{\partial t^2} = -\left[\frac{\partial u}{\partial t}\frac{\partial \eta}{\partial x} + u\frac{\partial}{\partial x}\left(-u\frac{\partial \eta}{\partial x}\right)\right],$$

which may be rearranged to give

$$\frac{\partial^2 \eta}{\partial t^2} = u^2\frac{\partial^2 \eta}{\partial x^2} - \frac{\partial \eta}{\partial x}\left(\frac{\partial u}{\partial t} - u\frac{\partial u}{\partial x}\right). \tag{2.3}$$

Substitution of eq. 2.2 and 2.3 into 2.1 gives

$$\eta_i^{n+1} = \eta_i^n - u\Delta t\left.\frac{\partial \eta}{\partial x}\right|_i^n + \frac{(u\Delta t)^2}{2}\left.\frac{\partial^2 \eta}{\partial x^2}\right|_i^n - \frac{(\Delta t)^2}{2}\left.\frac{\partial \eta}{\partial x}\right|_i^n\left.\left(\frac{\partial u}{\partial t} - u\frac{\partial u}{\partial x}\right)\right|_i^n. \tag{2.4}$$

If $\frac{\partial \eta}{\partial x}$ and $\frac{\partial^2 \eta}{\partial x^2}$ are evaluated to second order and the final term of eq. 2.4 is discarded, substitution of the finite-difference forms results in

$$\eta_i^{n+1} = \eta_i^n - \frac{1}{2}\left(\frac{u\Delta t}{\Delta x}\right)\left(\eta_{i+1}^n - \eta_{i-1}^n\right) + \frac{1}{2}\left(\frac{u\Delta t}{\Delta x}\right)^2\left(\eta_{i+1}^n - 2\eta_i^n + \eta_{i-1}^n\right), \tag{2.5}$$

which is second-order accurate in space and will be referred to as the "second-order" form. Note, however, that if u is not constant, the equation is only first-order accurate in time.

It is possible, although tedious, to develop, by similar methods, a form of eq. 2.5 which is fourth-order accurate in space. However, the "fourth-order" form so obtained remains only first-order in time. The finite-difference form is

$$\begin{aligned}\eta_i^{n+1} = \eta_i^n &- \frac{1}{12}\left(\frac{u\Delta t}{\Delta x}\right)\left[8\left(\eta_{i+1}^n - \eta_{i-1}^n\right) - \left(\eta_{i+2}^n - \eta_{i-2}^n\right)\right] \\ &- \frac{1}{24}\left(\frac{u\Delta t}{\Delta x}\right)^2\left[30\eta_i^n - 16\left(\eta_{i+1}^n + \eta_{i-1}^n\right) + \left(\eta_{i+2}^n + \eta_{i-2}^n\right)\right] \\ &+ \frac{1}{12}\left(\frac{u\Delta t}{\Delta x}\right)^3\left[2\left(\eta_{i+1}^n - \eta_{i-1}^n\right) - \left(\eta_{i+2}^n - \eta_{i-2}^n\right)\right] \\ &+ \frac{1}{24}\left(\frac{u\Delta t}{\Delta x}\right)^4\left[6\eta_i^n - 4\left(\eta_{i+1}^n + \eta_{i-1}^n\right) + \left(\eta_{i+2}^n + \eta_{i-2}^n\right)\right].\end{aligned} \tag{2.6}$$

THE CONSERVATION FORM

The one-dimensional form of eq. 1.4 is

$$\frac{\partial \eta}{\partial t} = \eta \frac{\partial u}{\partial x} - \frac{\partial (\eta u)}{\partial x} . \tag{2.7}$$

The transport term, $\partial(\eta u)/\partial x$, can be considered to be a divergence of a flux. By Green's theorem, any change in the advected quantity with time is proportional to the differential of flux across the boundaries. If the boundaries are established at points half the distance between grid points, then the flux at one of the boundaries is expressed by

$$F_{i+\frac{1}{2}} = (\eta u)_{i+\frac{1}{2}} = \frac{1}{\Delta t} \int_{x_{i+\frac{1}{2}}-u\Delta t}^{x_{i+\frac{1}{2}}} \eta(x')dx' . \tag{2.8}$$

If the variation of η is assumed to be linear within the zone, then integration of eq. 2.8 produces

$$F_{i+\frac{1}{2}} = \frac{\Delta x}{\Delta t}\left[\frac{1}{2}\left(\frac{u\Delta t}{\Delta x}\right)_{i+\frac{1}{2}}\left(\eta_{i+1} + \eta_i\right) - \frac{1}{2}\left(\frac{u\Delta t}{\Delta x}\right)^2\left(\eta_{i+1} - \eta_i\right)\right]. \tag{2.9}$$

If the variation of η is described by a cubic equation centered on the point, $i + \frac{1}{2}$, the resulting equation is

$$\begin{aligned} F_{i+\frac{1}{2}}\frac{\Delta t}{\Delta x} = {} & \frac{1}{16}\left(\frac{u\Delta t}{\Delta x}\right)\left[9(\eta_{i+1} + \eta_i) - (\eta_{i+2} + \eta_{i-1})\right] \\ & - \frac{1}{48}\left(\frac{u\Delta t}{\Delta x}\right)^2\left[27(\eta_{i+1} - \eta_i) - (\eta_{i+2} - \eta_{i-1})\right] \\ & - \frac{1}{12}\left(\frac{u\Delta t}{\Delta x}\right)^3\left[(\eta_{i+1} + \eta_i) - (\eta_{i+2} + \eta_{i-1})\right] \\ & + \frac{1}{24}\left(\frac{u\Delta t}{\Delta x}\right)^4\left[3(\eta_{i+1} - \eta_i) - (\eta_{i+2} - \eta_{i-1})\right], \end{aligned} \tag{2.10}$$

where the equation has been multiplied by $\frac{\Delta t}{\Delta x}$, and $\frac{u\Delta t}{\Delta x}$ is evaluated at $i + \frac{1}{2}$.

When $\frac{\partial u}{\partial x}$ is evaluated to second-order and the flux divergence is substituted for the transport term, the second-order difference form of eq. 2.7 is

$$\eta_i^{n+1} = \eta_i^n \left[1 + \frac{\Delta t}{2\Delta x}(u_{i+1} - u_{i-1})\right] - \frac{\Delta t}{\Delta x}(F^n_{i+\frac{1}{2}} - F^n_{i-\frac{1}{2}}), \tag{2.11}$$

where the form of the flux term is given by eq. 2.9.

Evaluation of $\frac{\partial u}{\partial x}$ to fourth-order and substitution of flux divergence as computed by eq. 2.10, results in the fourth-order finite-difference conservation form

$$\eta_i^{n+1} = \eta_i^n \left[1 + \frac{\Delta t}{12\Delta x}\{8(u_{i+1} - u_{i-1}) - (u_{i+2} - u_{i-2})\}\right] - \frac{\Delta t}{\Delta x}\left(F^n_{i+\frac{1}{2}} - F^n_{i-\frac{1}{2}}\right). \tag{2.12}$$

STABILITY CHARACTERISTICS

It is convenient to express the advective equations in terms of linear operators. Both forms of the advective equations described in this chapter have the same general equation,

$$\eta_i^{n+1} = \left[I\eta^n\right]_i - \left[A\eta^n\right]_i = \left[(I-A)\eta^n\right]_i, \tag{2.13}$$

where I represents the identity matrix and A represents the particular linear difference operator. Stability is, therefore, dependent on the eigenvalues of (I - A). Crowley [1] has shown that eqs. 2.5, 2.6, and 2.11 are stable for $\frac{u\Delta t}{\Delta x} \leq 1$, and that eq. 2.12 is stable for $\left(\frac{u\Delta t}{\Delta x}\right)^2 \leq 1.5$.

From Crowley's analysis of the amplitude and phase errors of the advection and conservation equations, the following generalizations are made:

1. Maximum amplitude damping and minimum phase retardation both occur at $\frac{u\Delta t}{\Delta x} \doteq 0.7$.
2. The rate of decrease in damping and of increase in phase retardation is greater for values of $\frac{u\Delta t}{\Delta x}$ larger than 0.7 than it is for values smaller than 0.7.
3. Amplitude damping and phase retardation are serious only for wave lengths shorter than four grid intervals.
4. The conservation form has slightly greater errors than the advection form in both amplitude and phase.
5. The fourth-order forms are clearly superior to the lower order forms in both amplitude and phase.

CHAPTER III

EXPERIMENTAL PROCEDURES

Both forms of the advective equation were developed for one-dimensional systems. Two-dimensional systems may be constructed by employing Marchuk's method of fractional time steps [1,3]. The linear operator form of such a system is

$$\eta_{i,j}^{n+1} = \left[(I-A)(I-B)\eta^{n}\right]_{i,j} \tag{3.1}$$

for the advection form, and

$$\eta_{i,j}^{n+1} = \left[(1-k)(I-A)(I-B)\eta^{n}\right]_{i,j} \tag{3.2}$$

for the conservation form. $A\eta$ and $B\eta$ represent the fluxes in the x and y directions respectively, and k represents the velocity divergence term in the conservation equation.

Using Marchuk's method, the final forms of the advective equations may be expressed as follows:

Advection form:

$$\begin{aligned} \eta_{i,j}^{*} &= \left[(I-B)\eta^{n}\right]_{i,j} \\ \eta_{i,j}^{n+1} &= \left[(I-A)\eta^{*}\right]_{i,j} \end{aligned} \tag{3.3}$$

Conservation form:

$$\begin{aligned} \eta_{i,j}^{*} &= \left[(1-k_y)(I-B)\eta^{n}\right]_{i,j} \\ \eta_{i,j}^{n+1} &= \left[(1-k_x)(I-A)\eta^{*}\right]_{i,j} \end{aligned} \tag{3.4}$$

The symbol, η^{*}, represents an intermediate value of the quantity at time n + 1, which results from the first one-dimensional step. Since each fractional step is, by itself, stable, the combination of the steps retains stability.

EQUATION CHARACTERISTICS TEST

The purpose of the initial experiment was to determine quantitatively, the performance characteristics of the several equations under known conditions which have some similarity to the atmosphere.

The grid system employed consisted of 3,969 points arranged in a square matrix of dimensions 63 x 63. The interval, d, between grid-points was approximately two hundred nautical miles. In this grid, the point with coordinates (31,31) lies exactly at the center, so that distances from the center are proportional to $[(31-i)^2 + (31-j)^2]^{\frac{1}{2}}$. For simplicity in this experiment, the surface was assumed to be flat; therefore no map factor was introduced.

A velocity field was generated which was proportional to the distance from the center point and which contained no shear (solid rotation). A pure divergent component was then added to the rotation. The resulting equations are

$$u = - My + Nx \ ,$$

and

$$v = \ \ Mx + Ny \tag{3.5}$$

where $x = (i-31)$ and $y = (j-31)$ are dimensionless coordinates. The first terms on the right are the rotational components and the second terms are the divergent components. M and N are arbitrary constants with units of meters per second, which determine the magnitude of the velocity components.

The initial field of the quantity to be advected consisted of a sinusoidal perturbation centered on grid-point (31,19) and zeroes elsewhere. The equation of the perturbation is

$$n_{i,j} = 10\left[1 - \sin\left(\frac{R\pi}{10}\right)\right], \quad R \leq 5, \tag{3.6}$$

where R = distance in grid intervals from point (31,19). Since d is approximately two hundred nautical miles, the perturbation has a maximum wave length of approximately two thousand nautical miles, which is of the same order of magnitude as the large scale vorticity disturbances.

The computer program was designed so that the angular velocity and the divergence could be varied in sign and magnitude as well as the number and length of time steps. Values representative of the atmosphere and forecast models were selected. The equation which relates the variables is

$$2\pi R_c d = MR_c S(\Delta t), \tag{3.7}$$

where

R_c = distance from grid center in grid intervals = 12,

d = length of grid interval = 3.81×10^5 meters,

S = number of time steps,

Δt = length of time step,

M = velocity factor (meters per second).

Preliminary calculations determined that with one-hour time steps, approximately two hundred steps would be required to advect the quantity through 2π radians with a realistic wind. The necessary velocity factor is

$$M = \frac{2\pi d}{S\Delta t} \doteq \frac{(6.28)(3.81\times10^5)}{(2\times10^2)(3.6\times10^3)} \doteq 3.32 \text{ m./sec.} \tag{3.8}$$

This factor produces a linear velocity of approximately forty meters per second at the point (31,19).

Initial experiments indicated that a suitable magnitude of N, the divergent factor, was 0.5 meters per second.

The scheme of the experiment was to advect the pattern through π radians with positive divergence, then to change the sign of the divergence for the remaining π radians. Assuming perfect advective properties, this method would return the pattern to its initial position and configuration after advection through 2π radians. Comparison of the initial and final patterns would show quantitatively errors in phase velocity and amplitude, as well as any computational instability which developed.

For purposes of comparison, eq. 1.3 was also subjected to the above conditions. The finite-difference form of eq. 1.3 which was used was

$$\eta_{i,j}^{n+1} = \eta_{i,j}^{n-1} - \frac{m\Delta t}{d}\left[u_{i,j}\left(\eta_{i+1,j}^{n} - \eta_{i-1,j}^{n}\right) + v_{i,j}\left(\eta_{i,j+1}^{n} - \eta_{i,j-1}^{n}\right)\right], \qquad (3.9)$$

which is second order in both space and time.

THE BAROTROPIC EXPERIMENT

The experiment just described subjects the advective equations to velocities which are linear in form and in comparison to the atmosphere, rather idealized. In order to test the advective equations under more realistic conditions, a simple form of the barotropic forecast model was chosen as follows:

$$\nabla^2 \frac{\partial \Psi}{\partial t} - \frac{\mu \bar{f}^2}{g\bar{Z}} \frac{\partial \Psi}{\partial t} = - F_a, \qquad (3.10)$$

where

Ψ = stream function
μ = constant = 4
$\bar{f}$ = average value of coriolis parameter = 1.03126×10^{-4} sec.$^{-1}$
$\bar{Z}$ = average value of 500-MB height = 5574 m.
F_a = advective forcing function = $\vec{V} \cdot \nabla\eta$.

The form of the linear balance equation employed to compute the stream function was

$$\nabla^2\Psi + \frac{1}{f}(\nabla\Psi\cdot\nabla f) = \frac{g}{f}\nabla^2 Z. \qquad (3.11)$$

However, the second term on the left in equation 3.11 was approximated by

$$\frac{1}{f}\left(\frac{g}{f}\nabla Z\cdot\nabla f\right),$$

reducing eq. 3.11 to a Poisson-type equation.

The scheme of the experiment consisted of equating the various forms of the advective equations to F_a. This could not be done directly since $F_a = \vec{V}\cdot\nabla\eta$, but by subtraction of $I\eta^n$ from both sides of eq. 2.13, the desired quantity was obtained as follows:

$$\eta^{n+1} - I\eta^n = -A\eta^n = \Delta\eta. \qquad (3.12)$$

The quantity $A\eta^n$ is substituted for F_a in eq. 3.10.

Two different methods were used to integrate the stream function in time. When the Jacobian was used as the forcing function in the prognostic equation, time integration of the stream function was accomplished by the leap-frog method. When the advection and conservation forms were used, time integration was done by forward steps, i.e.,

$$\Psi^{n+1} = \Psi^n + \frac{\partial\Psi}{\partial t}\Delta t\ , \qquad (3.13)$$

which is equivalent to eqs. 3.1, 3.2, 3.3, or 3.4.

PROGRAMMING PROCEDURES

All numerical computation required by this study was accomplished on the Control Data 6500 computer installed at Fleet Numerical Weather Central. FORTRAN, as modified for the CDC 6500, was the programming

language used. In addition to FORTRAN, several FNWC library subroutines were utilized.

No particular effort was expended to optimize the programs. Nevertheless, relative time requirements of the various methods should be significant.

During the construction of the computer program to solve the finite-difference equations, several minor modifications of the advective equations were necessary.

First of all, the boundaries of the grid necessitated the establishment of boundary conditions. The method chosen for the quantity, η, was simply to hold the boundary values constant. In the case of the fourth-order forms, the first interior value was computed using a second-order form.

Since the flux value was evaluated at half grid-points, and the boundary values of η were not allowed to vary, the first computation of flux occurred between the boundary point and the first interior point. This was accomplished with a second-order form in the fourth-order equations.

Similarly, the u and v components of the velocity field for the barotropic experiment were computed by second-order methods near the boundary, but in a different manner.

Since the u and v components are derived from the gradient of Ψ, it was possible to use fourth-order methods along the boundaries which were perpendicular to the separate velocity components. For the boundaries which were parallel to the components, a second-order form was used for the first interior value. This particular method was necessary because the conservation form includes interpolated velocity

components and a divergence term which requires the first derivatives of the velocity components.

The remaining modifications were due to the fact that the flux divergence term was computed for the points $i \pm \frac{1}{2}$ and $j \pm \frac{1}{2}$. Since the u and v components were computed for the interger points only, it was necessary to interpolate for the values at the intermediate points.

This was accomplished by using a linear interpolation on the perpendicular boundaries and a second-order interpolation elsewhere.

Fig. 1 shows the grid system employed in the conservation method.

Figure 1. Schematic of grid used in the conservation method. Integer grid-points are represented by + ; half-integer points by o.

CHAPTER IV

EXPERIMENTAL RESULTS

All contoured figures which appear in this chapter were produced by a California Computer Products, Inc , incremental plotter. The instructions to the plotter were computed by the CDC 6500 computer by a quadratic interpolation of grid-values. Contour labels on figures applicable to the linear advection experiment are proportional to the actual values. The contour origin, 0, corresponds to an actual value of -1.0 and the contour interval corresponds to 1.5 units.

To facilitate the discussion of the various advective equations, the following symbols will be used:

C4 denotes fourth-order conservation
A4 denotes fourth-order advection
A2 denotes second-order advection
JJ denotes common Jacobian

EQUATION CHARACTERISTICS TEST

The experiment consisted of advection of a pattern through 2π radians, about the center grid-point. This was accomplished in two hundred time steps of one hour each. The initial pattern and the resulting patterns after advection through π and 2π radians were plotted. Figs. 2-4 show the results when the fourth-order conservation equation was used. Fig. 5 and fig. 6 show the final results when the advection equations were used.

All methods show good results, considering that the final pattern represents the cumulative errors in advection of the pattern once around the earth at a velocity representative of a moderate jet stream.

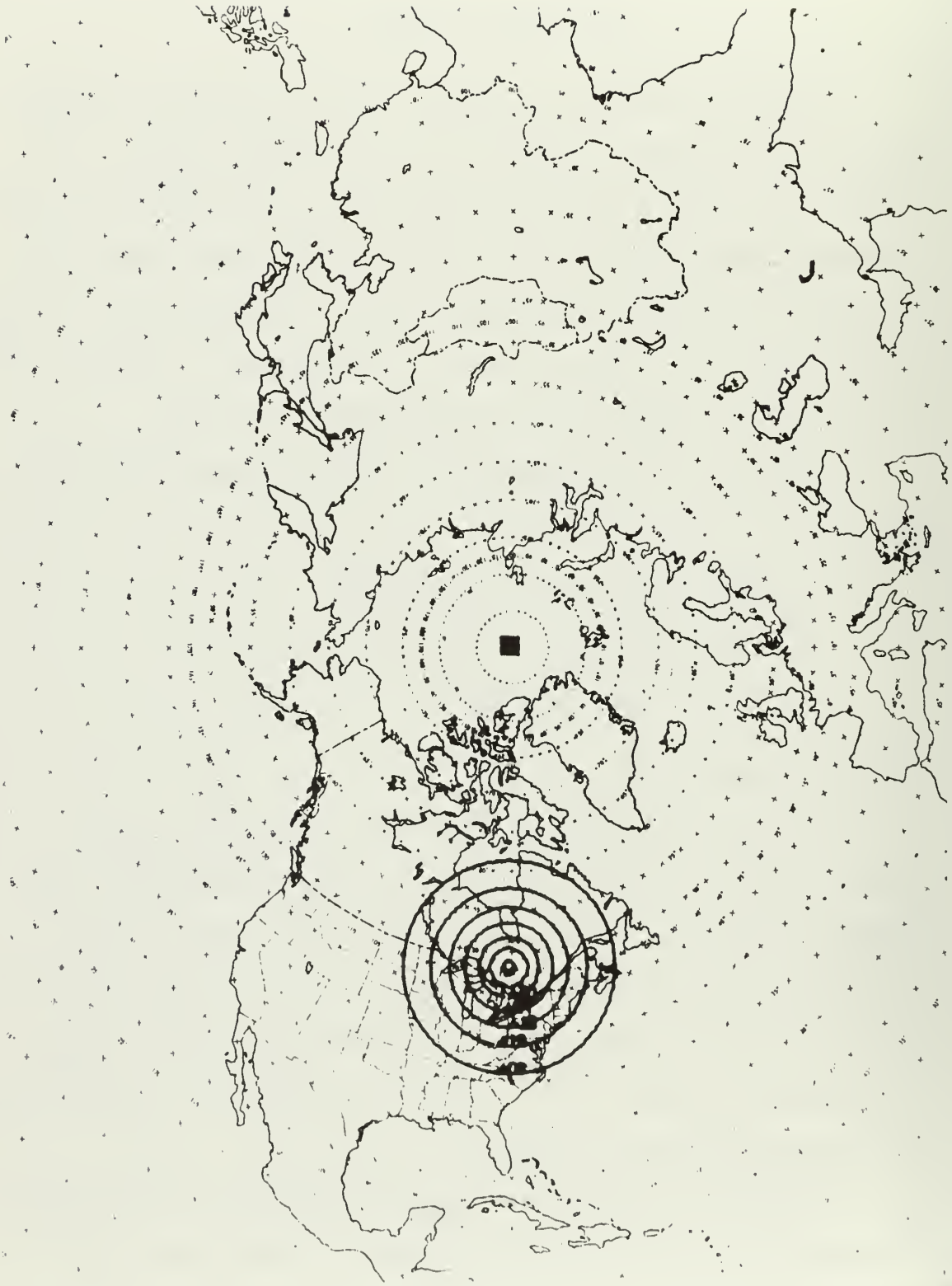

Figure 2. Contour plot of initial perturbation. Contour interval corresponds to 1.5 units; contour label 06 corresponds to 0.5 units.

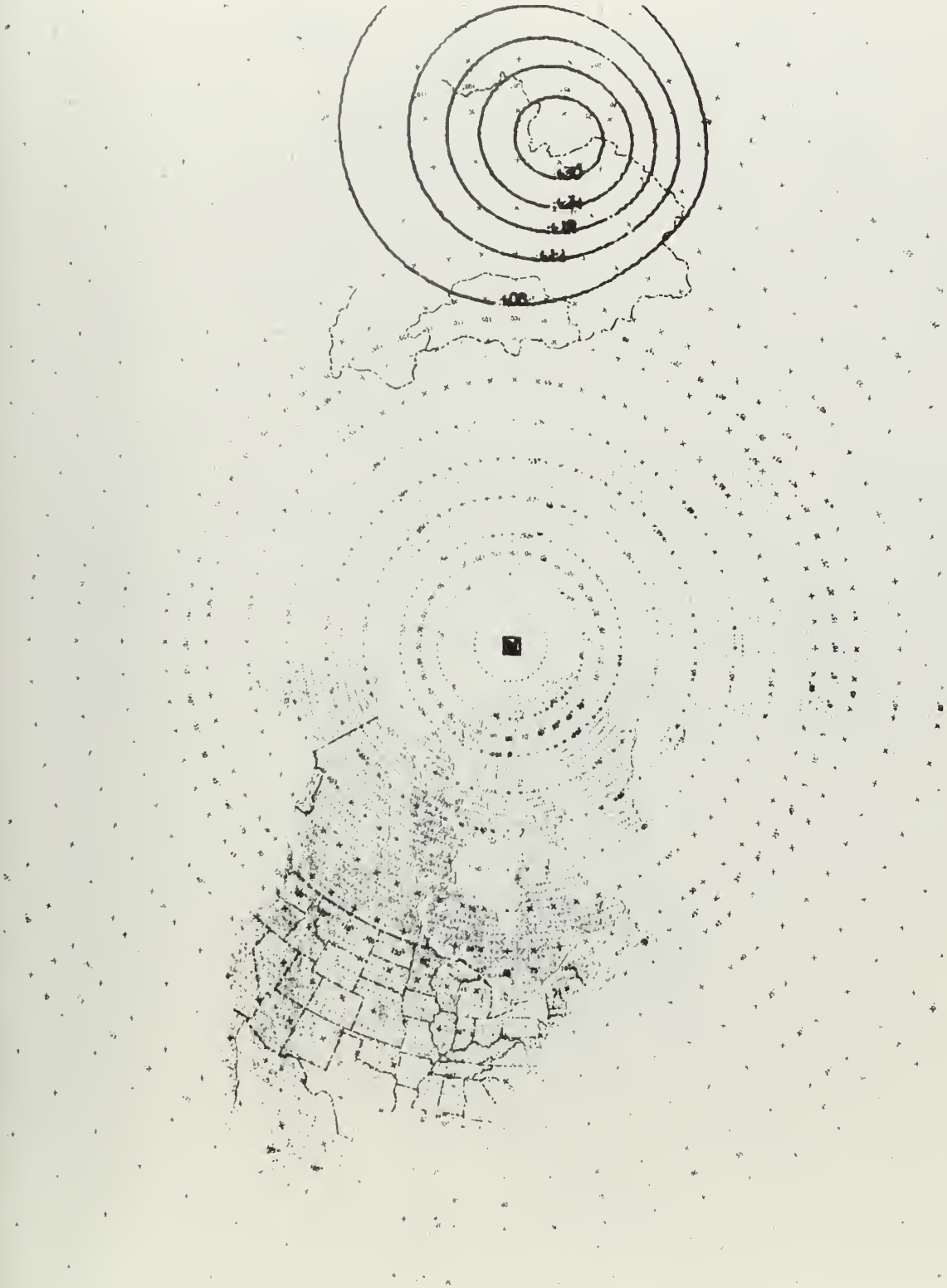

Figure 3. Plot of perturbation after 100 time steps by C4 method.

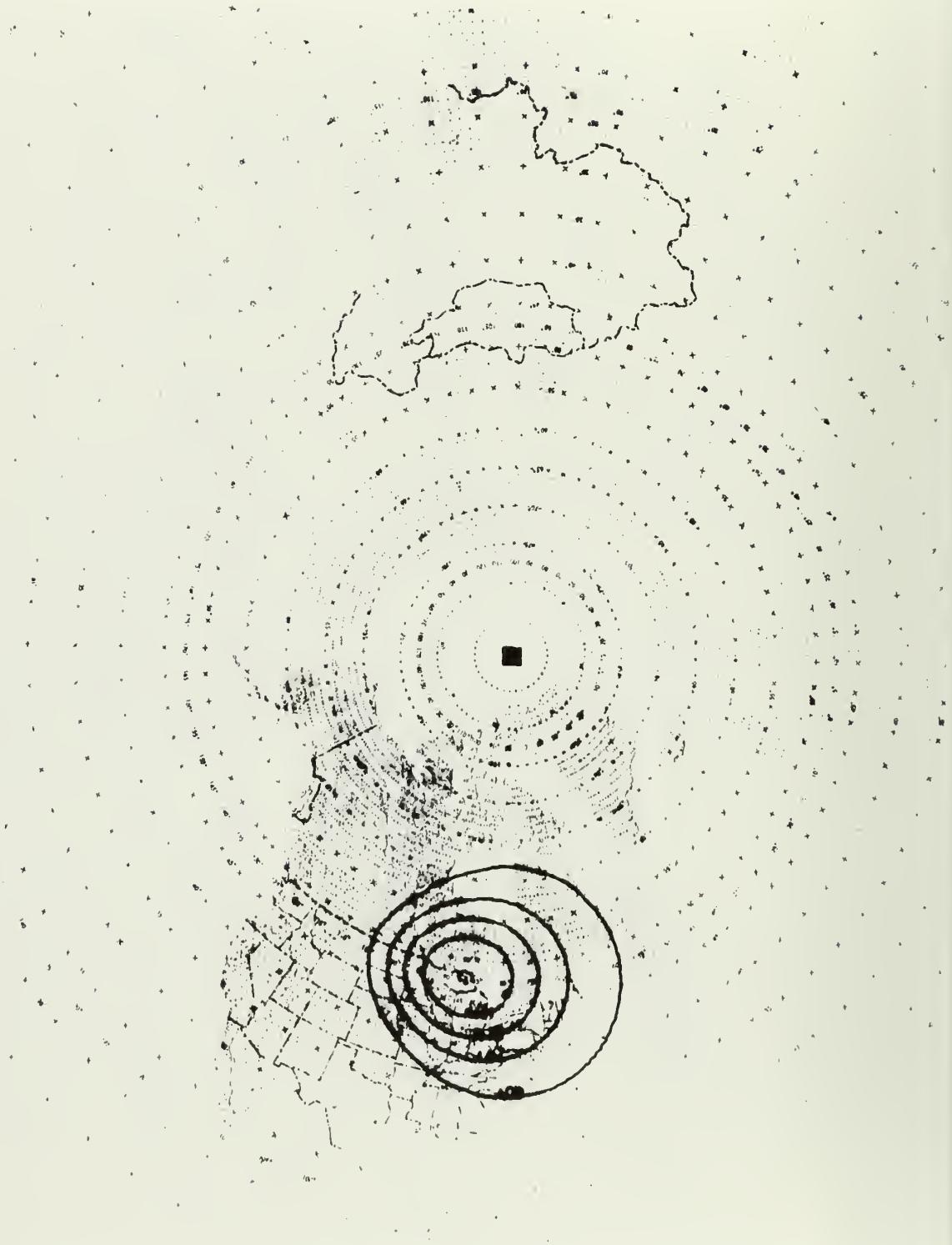

Figure 4. Plot of perturbation after 200 time steps by C4 method.

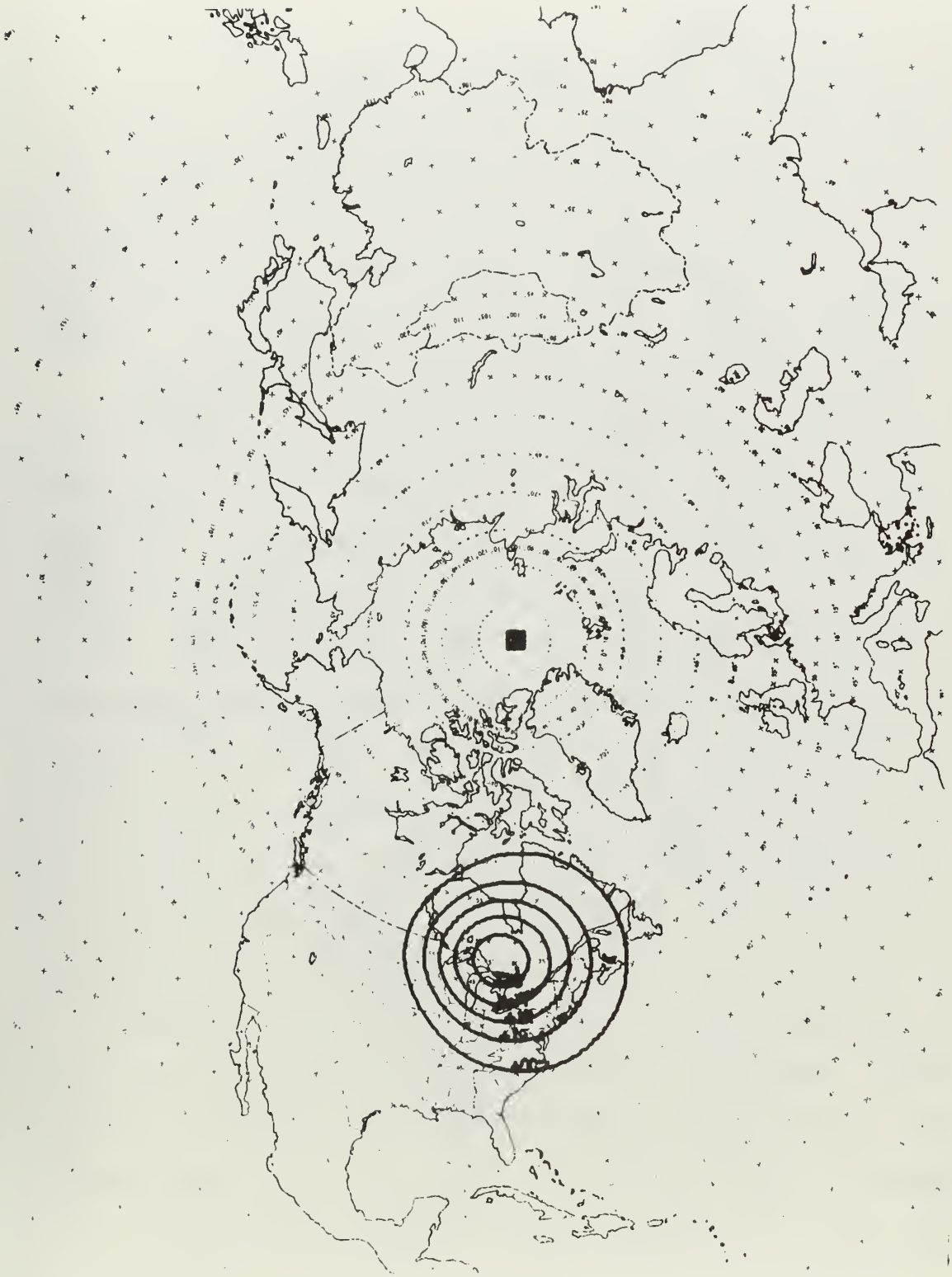

Figure 5. Plot of perturbation after 200 time steps by A4 method.

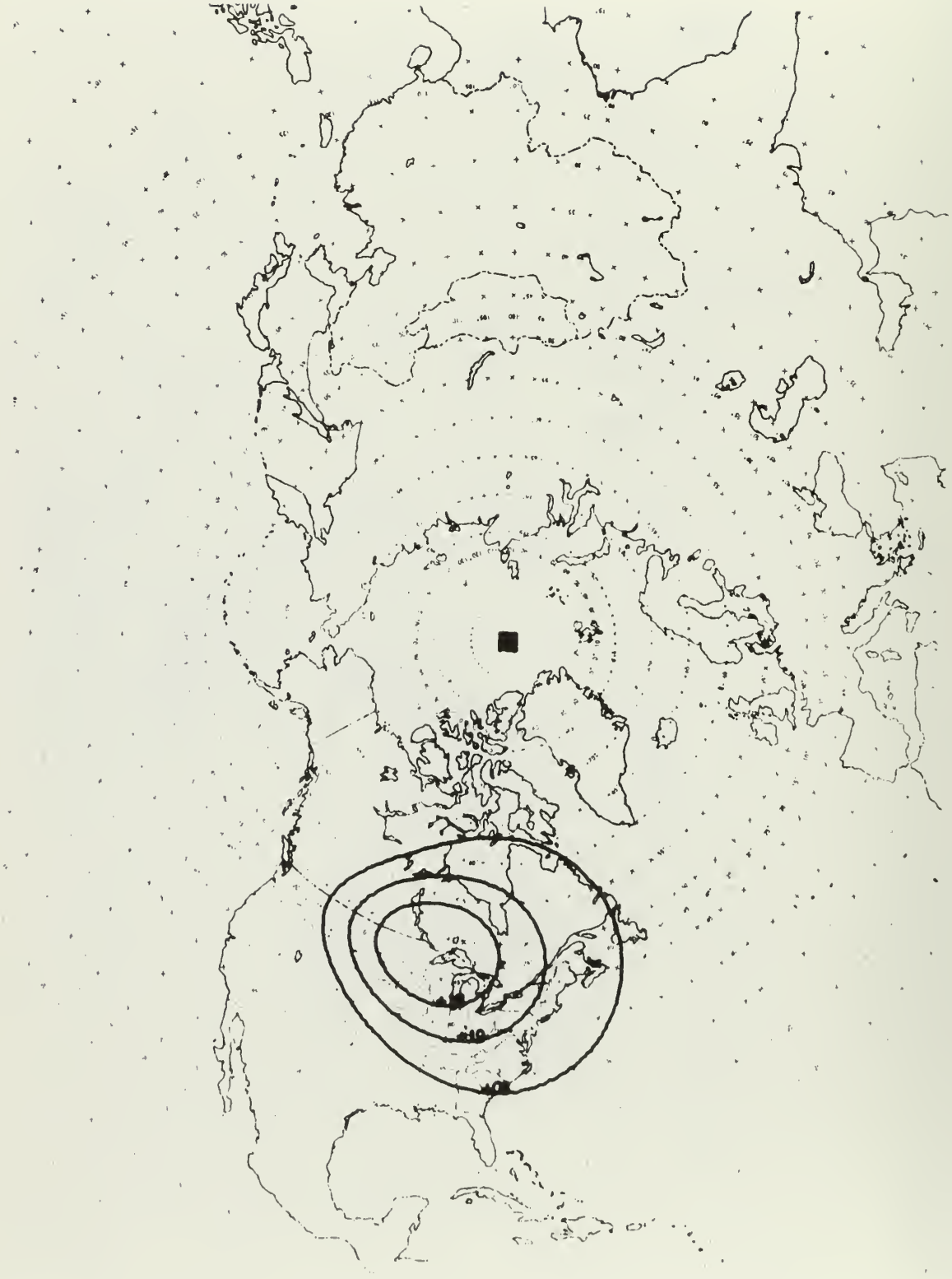

Figure 6. Plot of perturbation after 200 time steps by A2 method.

There are, however, significant quantitative differences. Table I shows the percentages of maximum error in phase and amplitude of each of the methods.

For purposes of comparison, the experiment was repeated using the J1 equation. Prior to the completion of one hundred steps, instability near the grid boundaries completely destroyed the pattern. This instability was eliminated by using one-half hour time steps. So that some reasonable comparison could be made between the methods, the number of time steps was doubled. The results are shown in fig. 7.

A particularly interesting result of the latter test was that after advection over approximately equal distances using twice the number of time steps, the amplitude error of the J1 result was less than that of the A2 method. On the other hand, the phase error was larger than that resulting from the A2 method.

All of the results were qualitatively consistent with Crowley's theoretical computations which were summarized in Chapter III. The eccentricity of the resultant patterns was apparently due to the wavelength sensitivity mentioned by Crowley. Support for this statement was provided by a comparison of the initial and final positions of the outermost contour in the forward semicircle; they were nearly coincident in both fourth-order results.

Although it is not apparent from the figures, small-amplitude noise was created by the advection and conservation methods. Nowhere did the amplitude of this noise exceed five percent of the magnitude of the perturbation. Except for the area close "behind" the pattern, the magnitude of the noise was less than one-half percent that of the perturbation.

TABLE I

PERCENTAGE OF MAXIMUM ERROR IN PHASE
AND AMPLITUDE OF
ADVECTIVE EQUATIONS

ADVECTIVE EQUATION	A4	C4	A2	J1
PHASE ERROR	0.67%	1.99%	3.45%	4.38%
AMPLITUDE ERROR	-25%	-34%	-51%	-48%

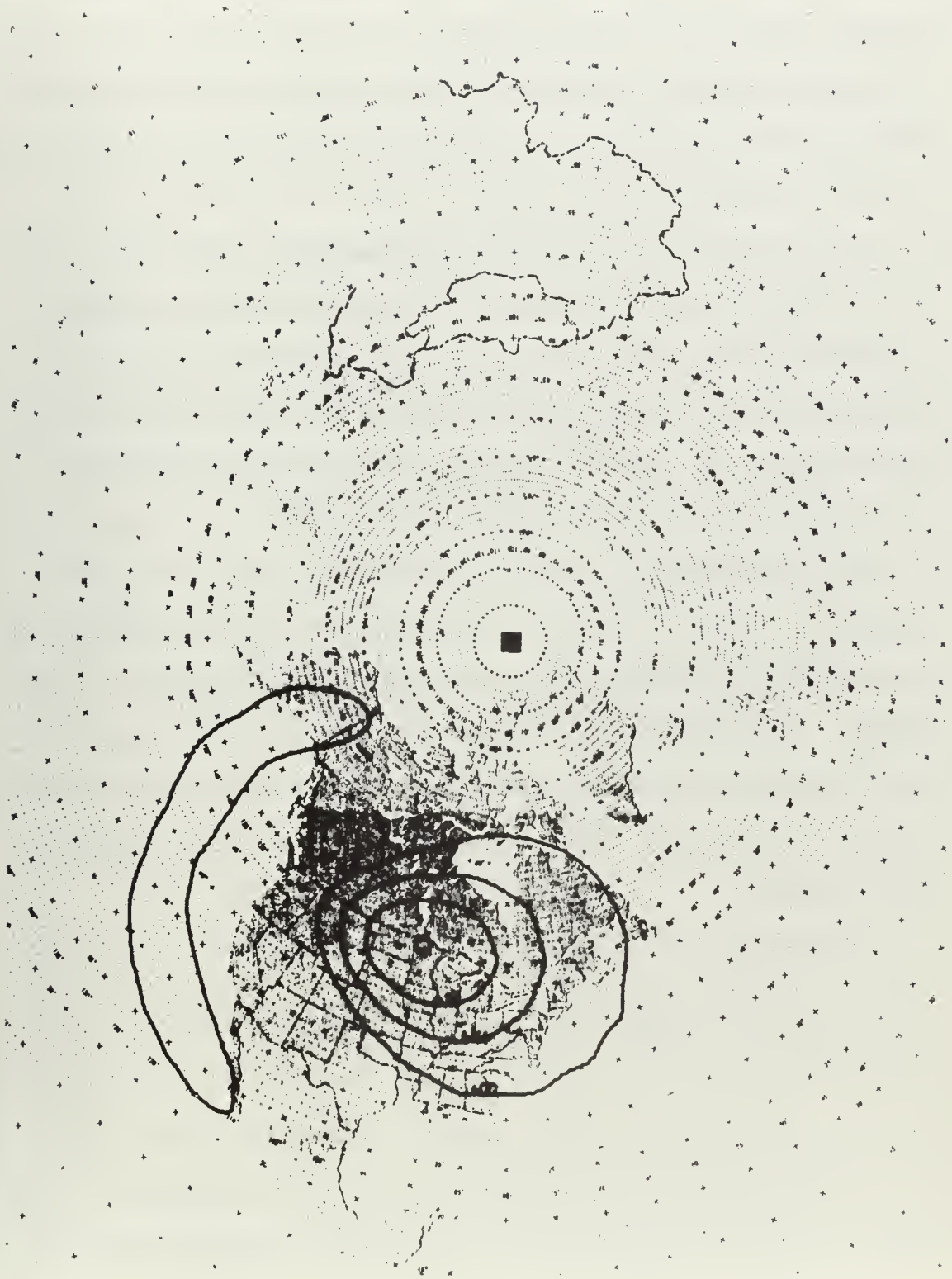

Figure 7. Plot of perturbation after 400 one-half hour time steps by J1 method.

A variation of the basic experiment was conducted to determine whether the length of the time step would have an effect. The time step was reduced to one-half hour and the number of time steps was doubled. The results obtained using the C4 method were nearly identical to those of the basic experiment. In this case, at least, any effect of reduction of the time step was apparently counteracted by the increased number of steps.

In his conclusions, Crowley [1] surmised that given a divergent velocity field, the performance of the conservation equation would be superior. He attributed the anticipated superiority to the explicit divergence term in the conservation form in contrast to the implicit divergence of the advection form. This experiment has not substantiated that supposition.

Computation time is usually a consideration in the design of atmospheric models. Obviously, the high-order schemes treated in this study require more computer time than the mathematically more simple schemes. Due to the "purity" of the computation in this experiment, it is possible to estimate, with high confidence, the relative requirements of the various forms by simply comparing the total computation time required.

If the time required by the J1 method is considered to be unity, then the relative "cost" of the other methods is listed below.

C4 = 5.14
A4 = 3.74
A2 = 1.98

It is obvious that the cost of the high-order equations in a pure advective model is considerable, but when these equations are used in

an iterative model such as the barotropic forecast model, the percentage increase in total time is small.

THE BAROTROPIC EXPERIMENT

The 500-MB analyses used in this experiment were produced by the Fleet Numerical Weather Central operational upper-air analysis program. Eight consecutive analyses beginning with 0000Z 15 January 1968 and ending with 1200Z 18 January were processed.

The choice of period was random except for the requirement that it be a winter period. As it turned out, it may have been an unfortunate choice because the upper air codes were changed on 1 January 1968. A comparison of the average number of 500-MB reports successfully decoded during the period of study with the average number successfully decoded during September 1968 results in the ratio, 330/374. It is possible, therefore, that one or more of the analyses contained significant errors.

Statistics on RMSE, pillow, variance of absolute vorticity, and mean absolute vorticity were computed for each map time. Contour maps of forecast values, and associated error maps, were produced for the following times only:

1200Z	15 January
0000Z	17 January
1200Z	18 January

The choice of these particular map times resulted from efforts to represent the extremes and mid-point of the period, and to avoid a multiple of twenty-four hours.

In addition to the statistics based upon the results of the various advective equations, RMSE and pillow were computed from the operational

prognoses of FNWC. Contour plots of the FNWC operational forecasts corresponding to the three time periods listed above were also produced.

Forecasts for twenty-four and forty-eight hours were produced. A one-hour time step was employed and no smoothing was applied to the forecasts produced by the advection and conservation equations.

Early in the experiment, it was found to be necessary to smooth the stream fields when employing the J1 equation, due to short-wave instability near the boundary. The method adopted was to apply a heavy smoother to the first four interior rows of grid-points on the initial stream field and on the forecast stream field at the twenty-four hour point. The boundary points and other interior points were not smoothed. The equation of the smoother is

$$\Psi_{i,j} = \frac{\Psi_{i+1,j} + \Psi_{i-1,j} + \Psi_{i,j+1} + \Psi_{i,j-1}}{4} \qquad (4.1)$$

This smoother was probably excessive, but no significant activity occurs south of 13°, the most northerly latitude of the smoothed points. The smoothing resulted in a significant reduction of σ_η^2, however.

Table II shows the RMSE which resulted from the forecasts produced by the C4, A4, A2, and J1 equations, and the FNWC operational forecasts. Means and standard deviations for the eight map times are also shown.

Although RMSE is certainly not a conclusive measure of forecast skill, it is usually an indication of the relative accuracy of various methods. Table II suggested that in this experiment, skill was inversely proportional to the complexity of the advection equation employed in the model. This was indeed disturbing. Furthermore, it is surprising to note that all methods except C4, without smoothing,

TABLE II

RMSE IN METERS OF VARIOUS FORECAST METHODS

MAP TIME	C4		A4		A2		J1		FNWC	
	24 HR	48 HR	24 HR	48 HR	24 HR	48 HR	24 HR	48 HR	24 HR	48 HR
15/0000Z	47.4	81.3	44.1	77.2	43.5	74.0	37.9	67.3	43.0	74.8
15/1200Z	45.6	72.2	43.9	70.8	41.7	65.7	40.1	62.3	45.1	71.1
16/0000Z	39.2	74.5	39.9	70.0	38.7	69.0	37.6	64.6	42.6	73.9
16/1200Z	45.4	84.7	41.4	75.5	40.8	76.1	37.8	71.0	44.0	80.2
17/0000Z	49.3	83.9	44.6	71.7	44.4	70.5	40.9	66.5	48.4	78.1
17/1200Z	46.5	78.9	46.3	70.5	45.7	69.9	41.5	64.3	46.4	70.9
18/0000Z	48.0	78.7	44.3	64.6	44.8	65.8	40.2	60.5	43.7	67.2
18/1200Z	45.2	74.6	38.4	59.8	37.5	58.0	35.8	53.0	40.8	69.9
Mean	45.8	78.6	42.9	70.0	42.1	68.6	39.0	63.7	44.3	73.3
STD DEV	2.84	4.28	2.51	5.22	2.78	5.23	1.85	5.02	2.21	4.07

surpassed the skill of the FNWC operational model, which is considerably more complex than the model utilized in this experiment.

To resolve this apparent paradox, the various prognostic charts and their associated error charts were compared with the verifying analyses. From this analysis the following conclusions were drawn:

1. Closed lows existing on the analysis continued to deepen when C4 and A4 equations were used. When all methods continued the deepening process the C4 and A4 equations showed the highest rate of deepening. Frequently, these lows showed filling on the verification maps.
2. Movement of low centers was more rapid in the C4 and A4 results, and usually more accurate when the low moved rapidly.
3. Trough movements were significantly larger in the fourth-order results than they were in the results of the low-order equations. Frequently, the trough movement forecast of the A4 and C4 equations exceeded the actual movement in the vicinity of the jet stream.
4. None of the methods were successful in the development of a low-latitude cut-off low; a typical barotropic model failure.
5. The southern extremity of all short-wave troughs, except those of FNWC, showed considerable lag. Considering this fact, the overall movement of troughs appeared to be the best in FNWC progs. Note, however, that FNWC has incorporated a modification tested by Lewit [4] to accelerate low-latitude troughs.

From these conclusions, the inverse relationship of RMSE is at least partially explained. They do not, however, explain why RMSE of FNWC progs was large. Examination of the error charts showed that in general, FNWC error centers were smaller than those in the experimental methods. In the Pacific Ocean west of the Hawaiian Islands and over eastern Asia, however, FNWC errors were consistently larger than those in the experimental methods. A large positive error center in the

central Pacific and a moderate negative error over eastern Asia persisted on all FNWC charts. The Pacific error center appeared on charts of the experimental methods, but was of lower intensity. The negative error over Asia was absent in the experimental methods. No explanation was found for this inconsistency.

Although generalizations were helpful in the explanation of the RMSE, they may not represent the characteristics of the model in a given forecast situation. A detailed analyses of the 15/1200Z map time was conducted to determine the qualitative and quantitative differences in performance of the models.

The 15/1200Z map time was chosen because (1) the report count was the largest of all map times in the series, (2) the report count for the verification time, 16/1200Z, was well above average, and (3) the RMSE of the various methods closely approximated the mean values for all eight periods.

Fig. 8 is a contour plot of the 15/1200Z analysis. It is typical of a rather low-index pattern with a nearly symmetrical blocking situation in the central Pacific and deep troughs over the eastern United States, eastern Atlantic, and eastern Europe

Fig. 9 is a plot of the 16/1200Z analysis, which provided the verification for the prognoses. It is apparent that little change has occurred in the Pacific hemisphere, but that the movement of short waves in the Atlantic hemisphere has caused changes sufficient to exercise the forecast models.

Figs. 10-14 are plots of the twenty-four hour progs produced by each of the methods. The most striking feature of these figures is the smoothness of the advection and conservation methods compared to

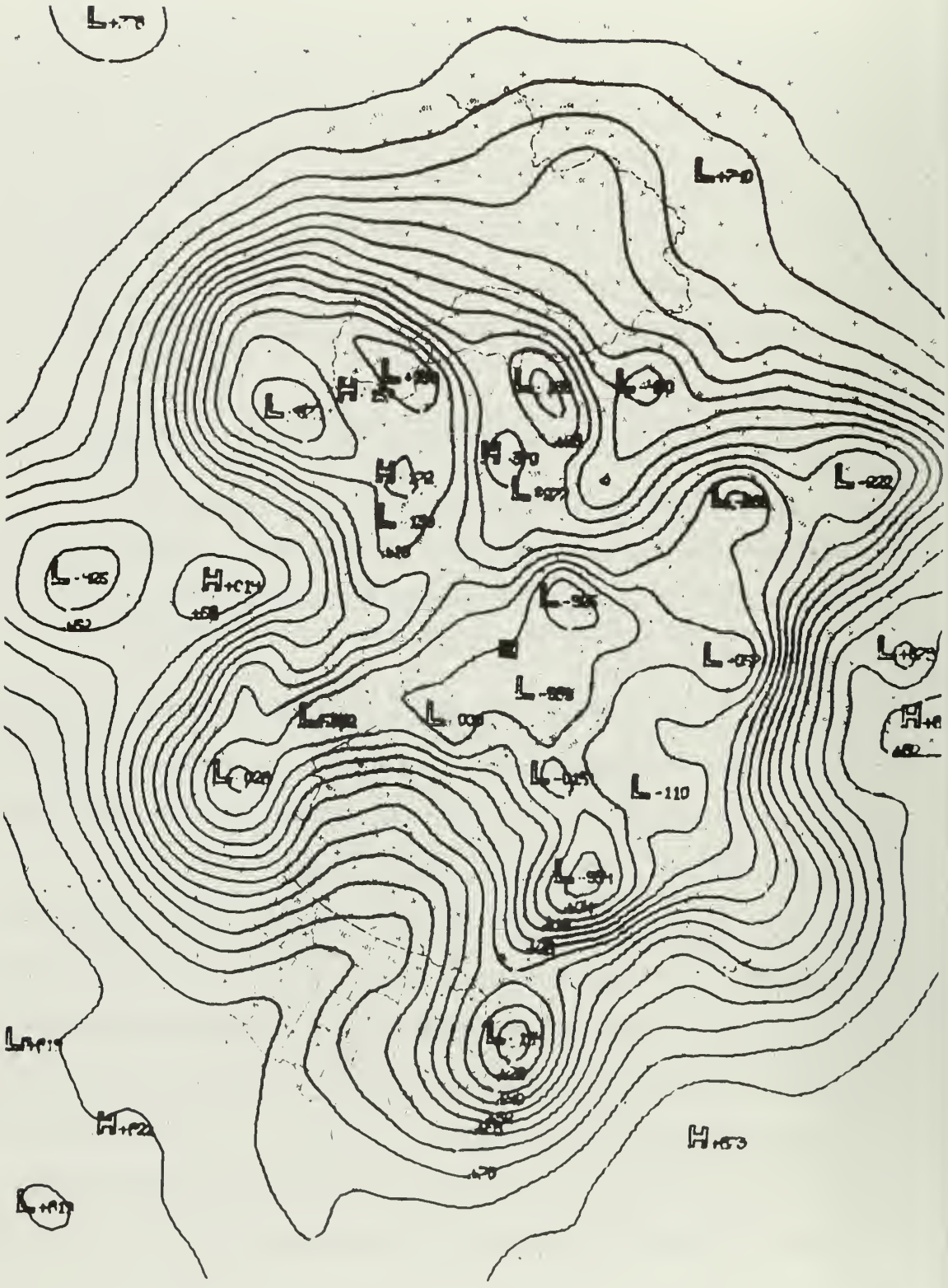

Figure 8. FNWC height analysis at 500-MB for 1200Z 15 January 1968. Contour interval is 60 meters.

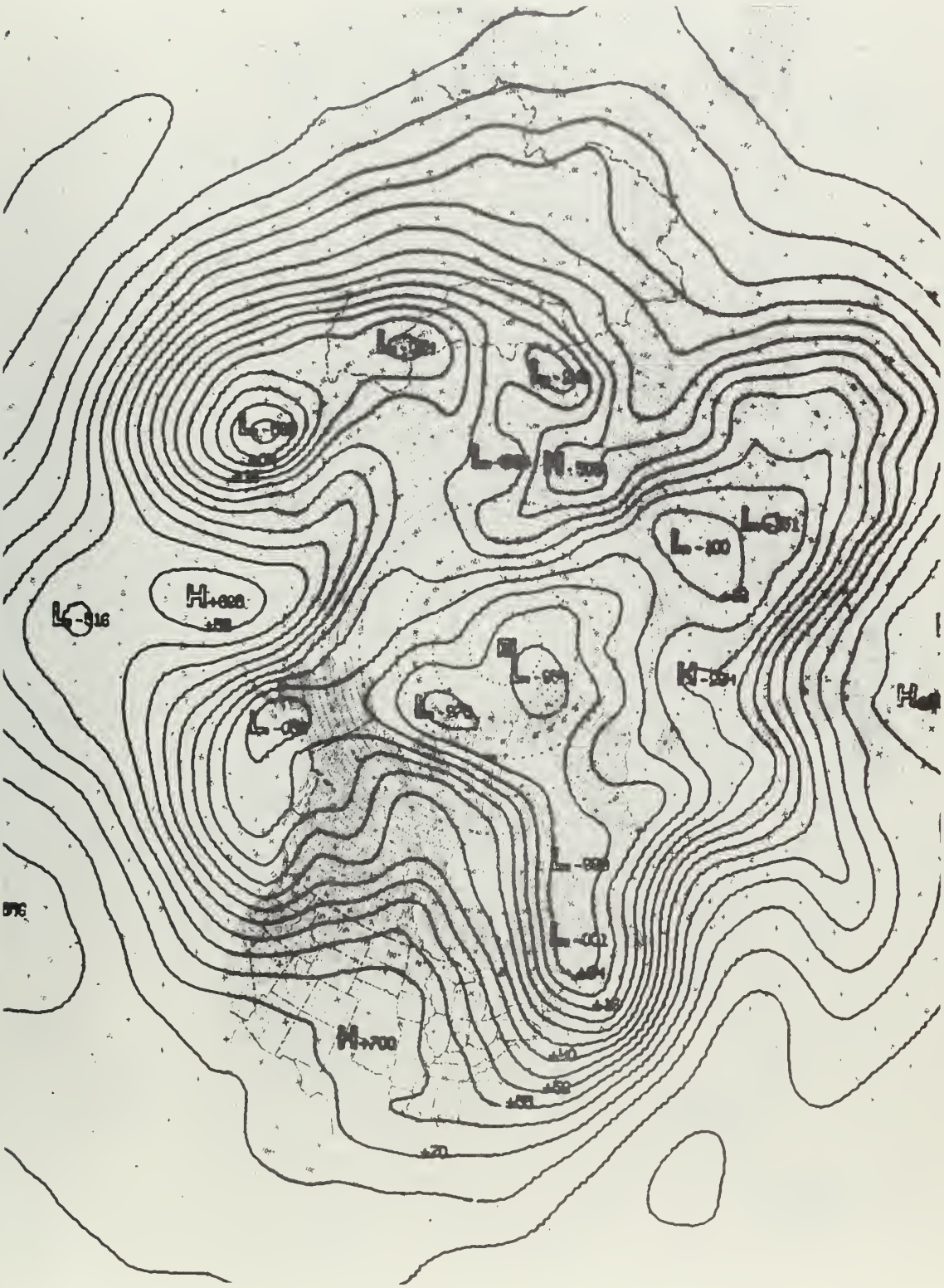

Figure 9. FNWC height analysis at 500-MB for 1200Z 16 January 1968.

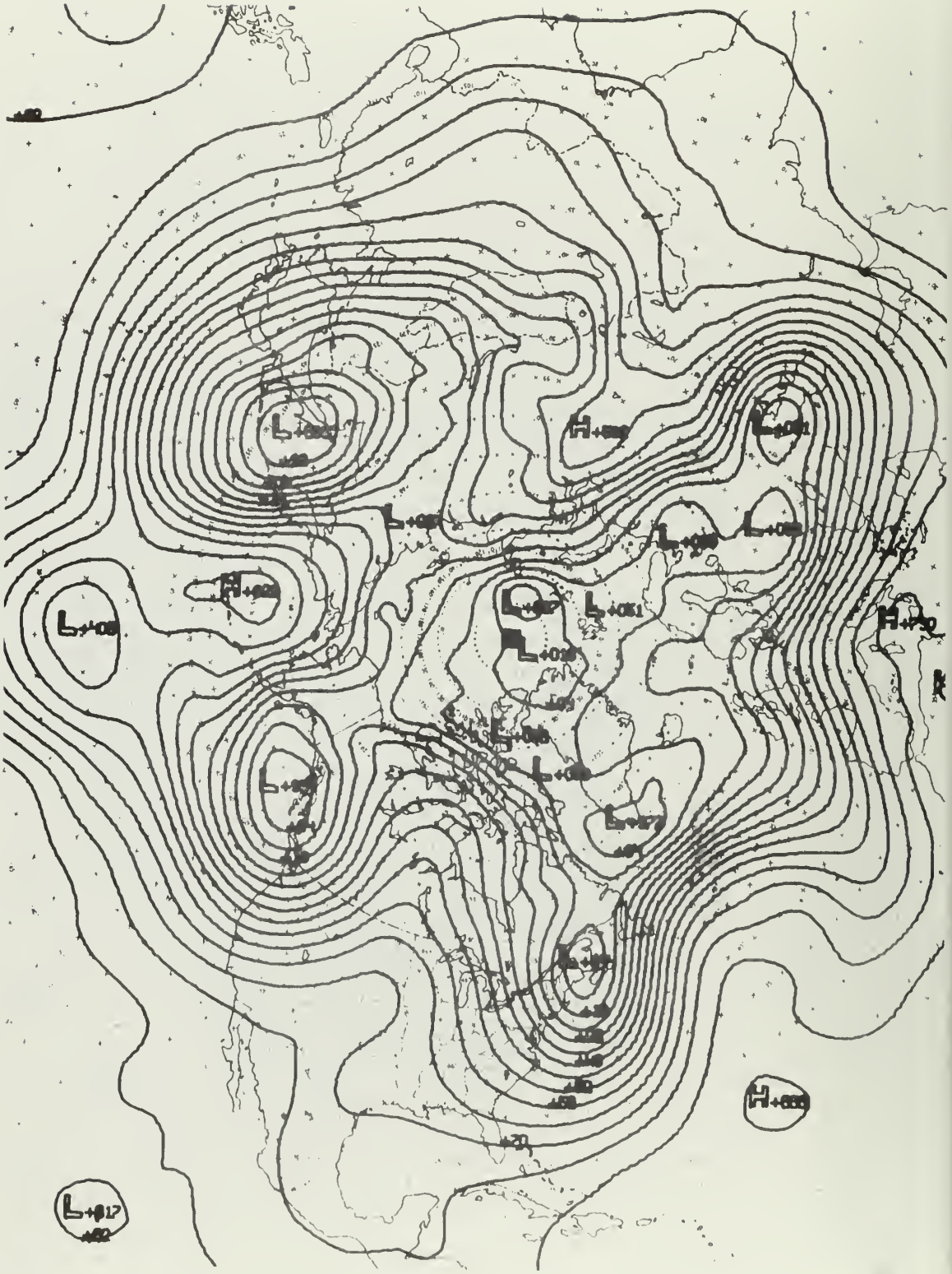

Figure 10. C4 24-hour 500-MB prog verifying 1200Z 16 January 1968.

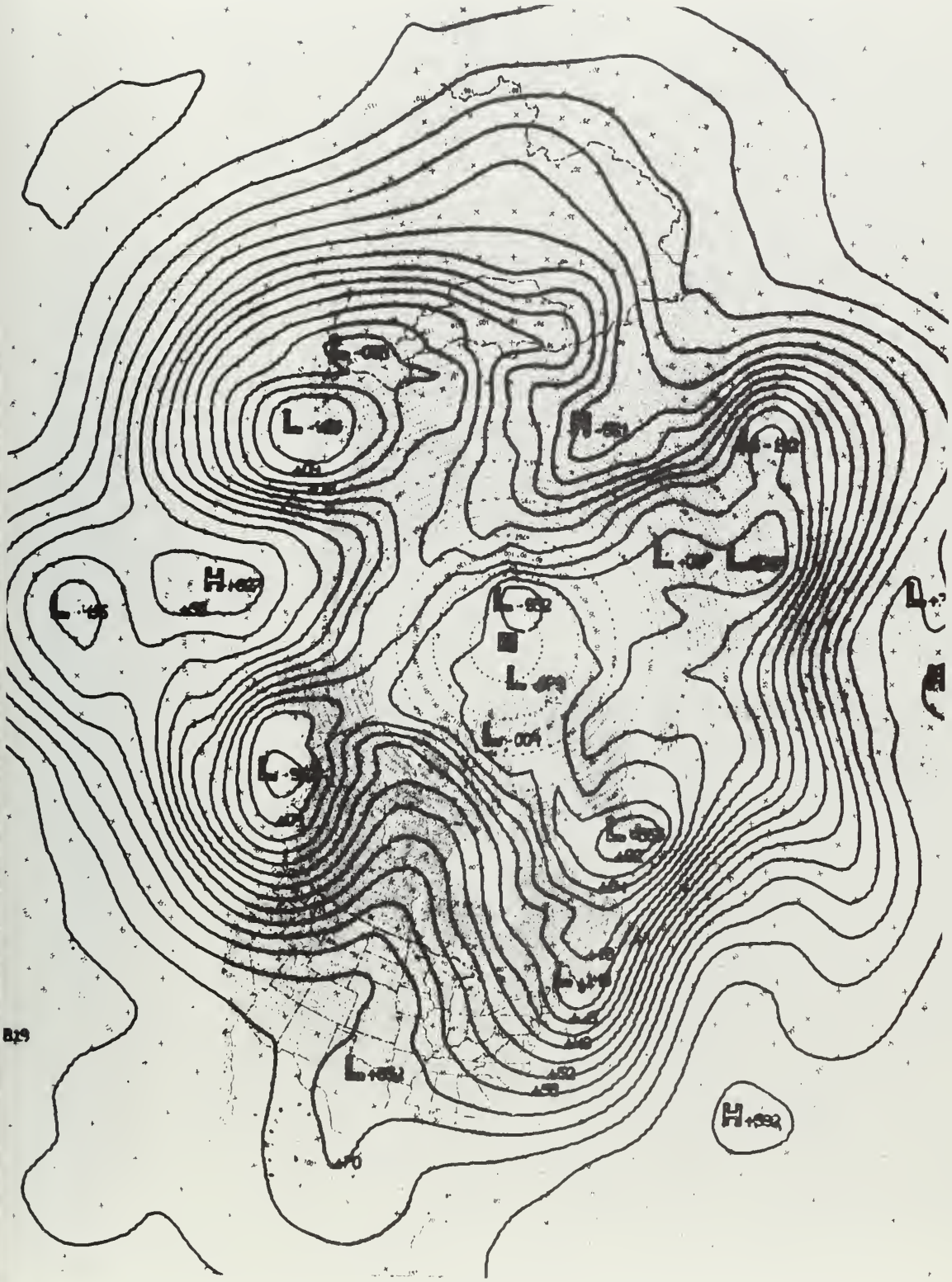

Figure 11. A4 24-hour 500-MB prog verifying 1200Z 16 January 1968.

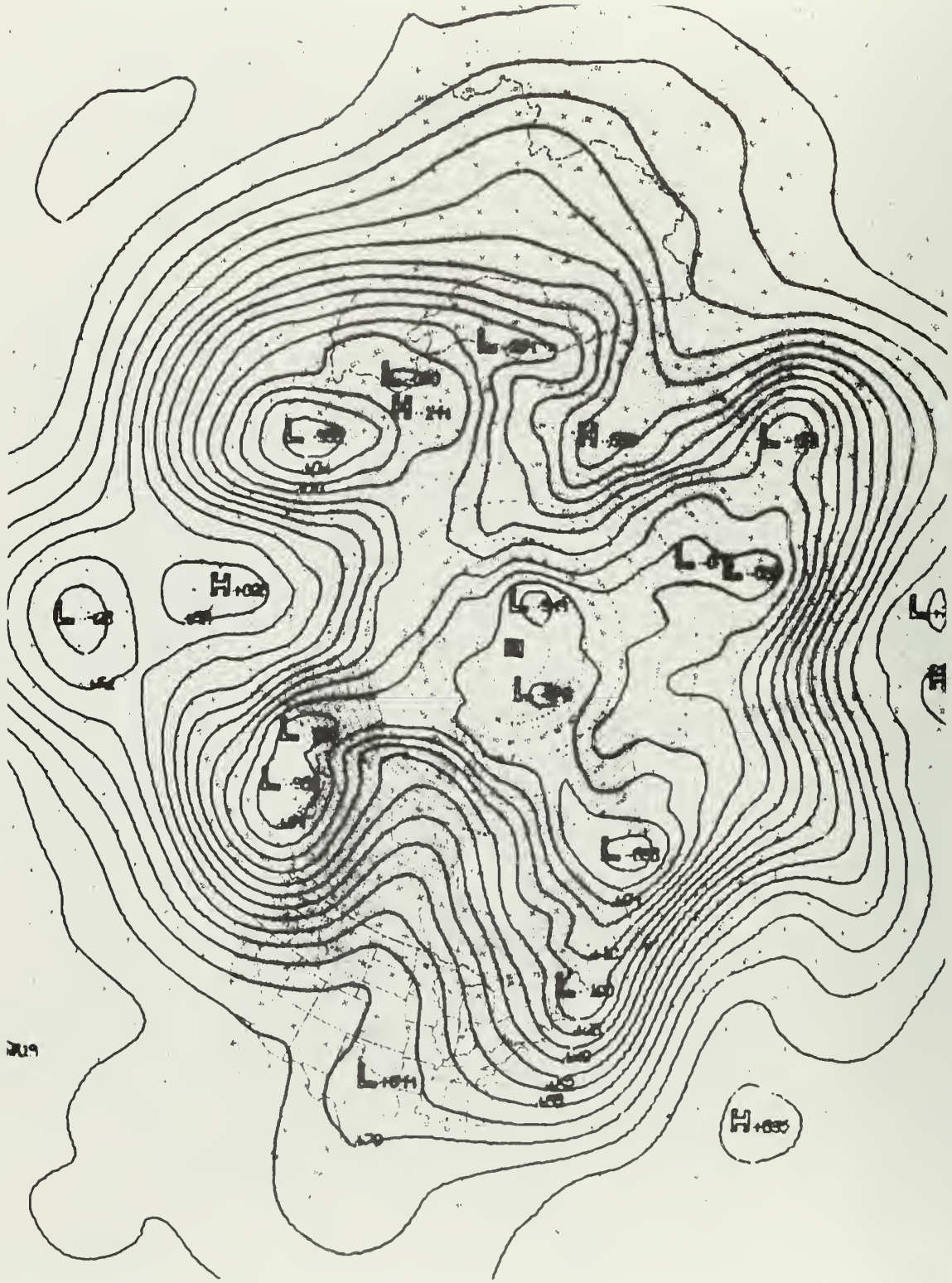

Figure 12. A2 24-hour 500-MB prog verifying 1200Z 16 January 1968.

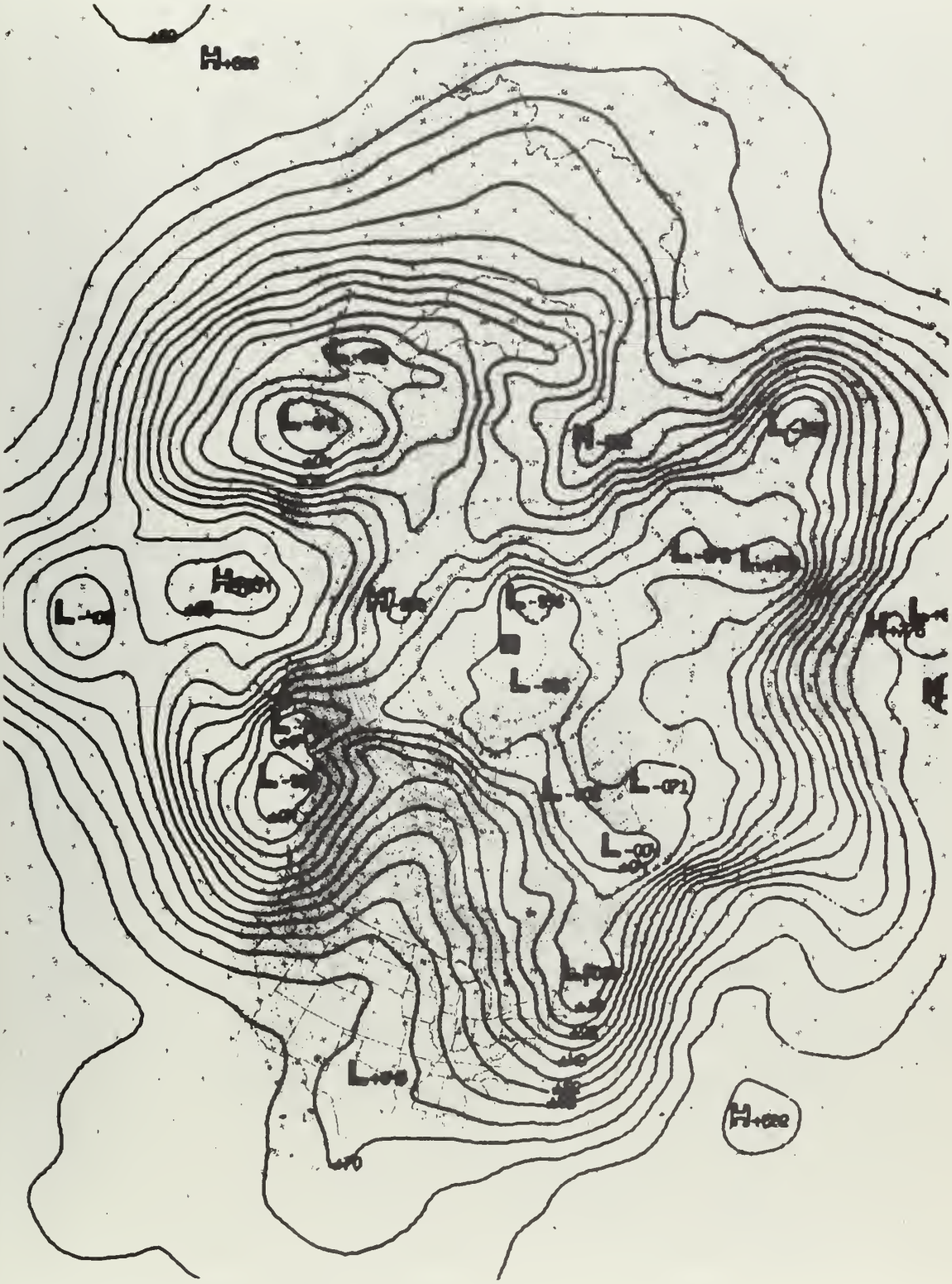

Figure 13. J1 24-hour 500-MB prog verifying 1200Z 16 January 1968.

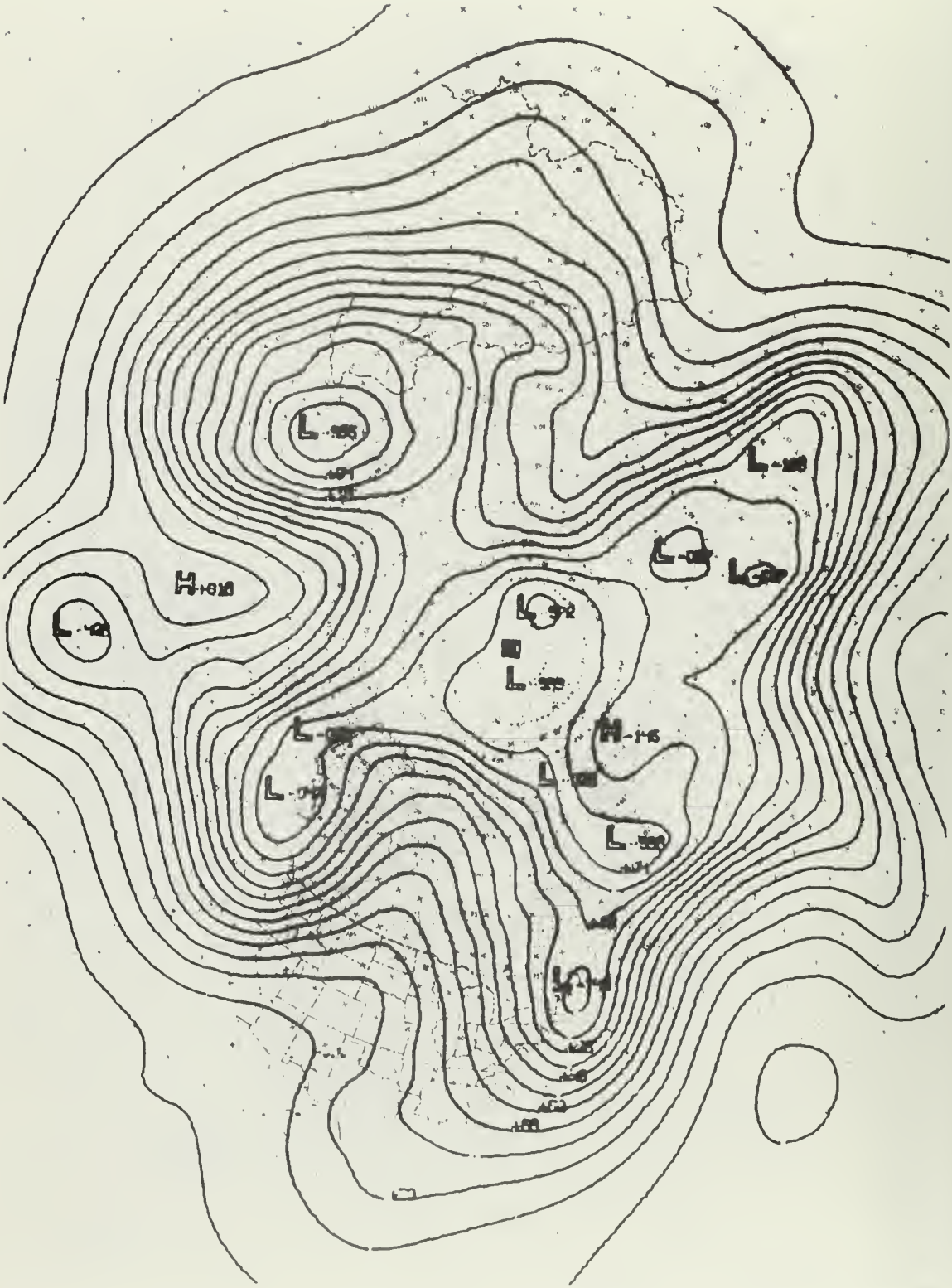

Figure 14. FNWC 24-hour prog verifying 1200Z 16 January 1968.

the J1 method. This is a consistent feature. The smoothness of the FNWC prog is a result of repeated smoothing during the integration process.

The trough over Labrador and associated ridges to the east and west appear to have been handled best by the C4 method. The FNWC prog is nearly as good in position and shape but has a much larger error in central pressure. This is a deepening situation.

Large differences occurred in the handling of the low which, in the analysis, is located off the northeast Labrador coast. This low filled by verification time. The J1 method and FNWC excelled in this case. Note that the Crowley methods moved this feature northeastward and the A4 and A2 methods deepened it. Contrary to the generalization made earlier, the C4 method showed slight filling.

The trough in the eastern Atlantic was handled rather well by all methods, but the J1 method appears to have the best shape. Note that the A4, C4 and FNWC methods all move the trough too rapidly in the higher latitudes.

The weak low located over southern Norway is of particular interest, since it is the only rapidly moving low on the chart. It can be followed to a position approximately 300 miles north of the Black Sea by verification time. The movement forecasted by the C4 method is clearly superior, but the central pressure is in error by more than 120 meters, which is more than twice the error shown in the FNWC prog.

The deep trough near the Caspian Sea was handled poorly by all methods. The fourth-order methods are particularly bad because of excessive deepening, especially the C4 method. Central Asia was handled similarly by all methods with only small differences in detail. The FNWC prog, however, appears to be overly smooth.

Although there appeared to be but small differences in the handling of the deep low north of Japan, the strong gradient produced quite different error patterns. The low moved northeast and deepened. The J1, A4 and A2 methods moved it north. The FNWC prog resulted in movement slightly west of north. The C4 prog was clearly superior in the movement and deepening of this center, but also had an excessive northerly component.

Since the western Pacific area was particularly difficult for the FNWC prog, it was interesting to compare the error charts of the FNWC prog with the C4 prog in this area. Fig. 15 and fig. 16 are computations of prog minus verification, contoured at intervals of sixty meters. The differences are quite significant.

All methods treated the blocking situation similarly. All failed to reduce the intensity of the low to the value shown on the verification. Note, however, that the low is positioned in a sparse data area. It is quite possible that the center was more intense than indicated by the analysis.

No significant differences in the handling of the Gulf of Alaska cyclone were apparent.

The foregoing analysis of movements and intensities has indicated that no single method was always best. The C4 method usually gave best results when a system was intensifying or moving rapidly, but the FNWC prog, and often the low-order progs, appeared to give best results when the system was static or weakening.

Investigation of the forecasts produced from the 17/0000Z and 18/1200Z maps indicated that the above conclusions are applicable to other map times of this series. It does not follow, however, that

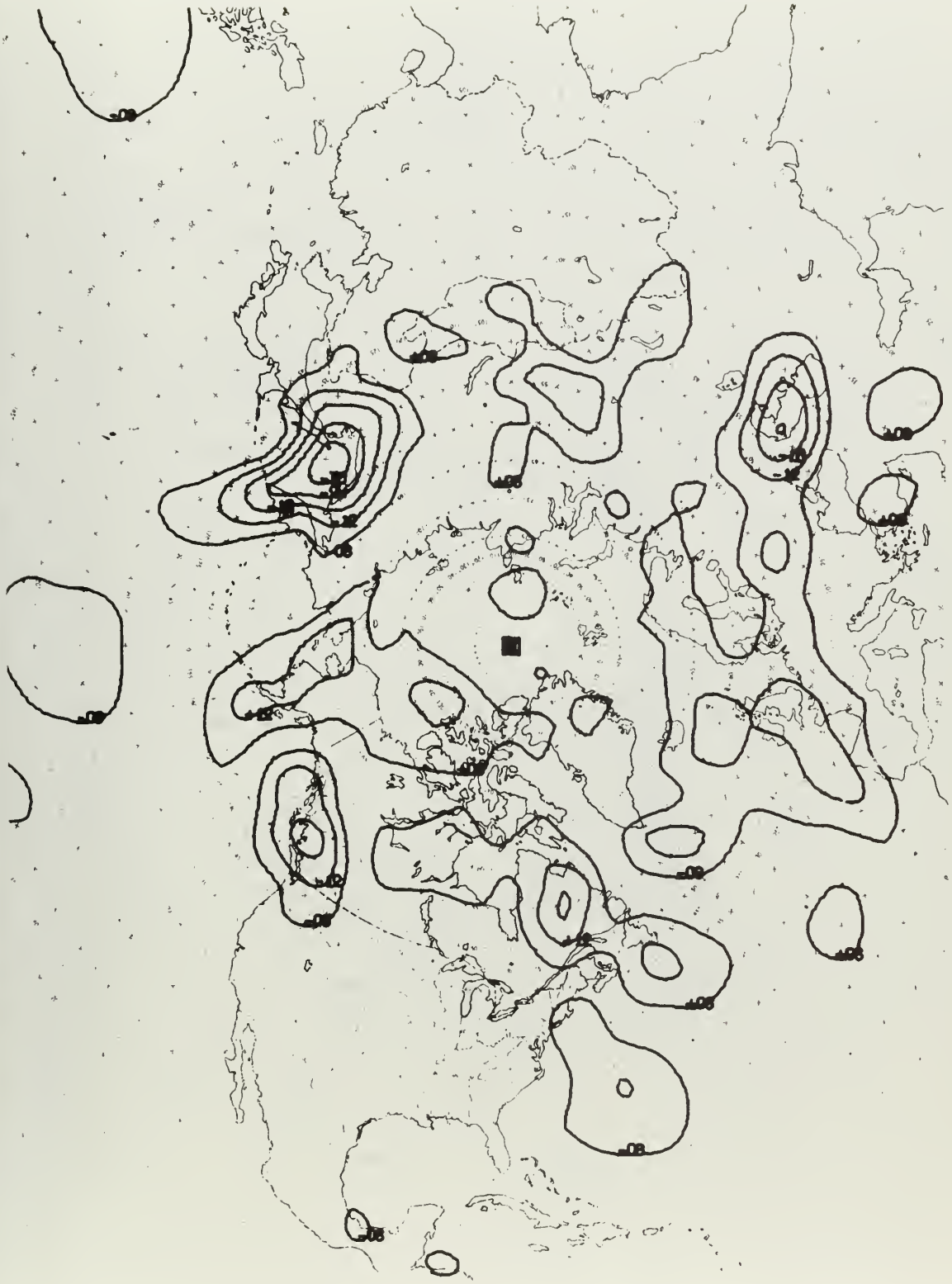

Figure 15. C4 24-hour 500-MB prog error. Contours are prog minus verifying analysis. Contour interval is 60 meters.

Figure 16. FNWC 24-hour 500-MB prog error.

these conclusions are applicable to all situations of the atmosphere. High-index situations, for example, might be troublesome, although the high-order methods appeared to excel when forecasting large movement. Weak, summertime gradients might result in errors which are not apparent in this series. There is little doubt, however, that the advection and conservation equations remain stable in typical meteorological wind fields. Moreover, the theoretical phase and amplitude characteristics appear to remain valid for these fields.

CHAPTER V

SUMMARY

Second-order and fourth-order advection equations have been developed for one dimension in conservation and advection forms. These equations have previously been shown to be stable for forward time steps when $\frac{u\Delta t}{\Delta x} \leq 1.0$, and in the case of the fourth-order conservation form, when $\left(\frac{u\Delta t}{\Delta x}\right)^2 \leq 1.5$.

Phase retardation was also shown to be a minimum and amplitude damping a maximum for $\frac{u\Delta t}{\Delta x} \doteq 0.7$. The advection form demonstrated somewhat better phase and amplitude characteristics than the conservation form.

Use of Marchuk's method of fractional time steps permitted the one-dimensional equations to be applied to a two-dimensional finite-difference scheme without loss of stability or modification of phase and amplitude characteristics.

In this study a controlled experiment utilizing a divergent, but linear velocity field was conducted. A known pattern representative of a simplified atmosphere was advected through 2π radians by a velocity field of magnitude comparable to the atmosphere. Two hundred time steps were required.

Positive, constant divergence was applied during the initial one hundred time steps; then negative divergence of equal magnitude was applied during the final one hundred steps. The object of the experiment was to determine how well the initial pattern was conserved. Crowley's theoretical stability analysis was substantiated by the experiment.

With a one-hour time step, computational instability of the Jacobian form destroyed the field before advection through π radians could be accomplished. Reduction of $\frac{u\Delta t}{\Delta x}$ to one-half of the value used in the basic experiment and doubling the number of time steps eliminated the instability. It was found that the Jacobian form had better amplitude characteristics than the second-order advection method, but that the phase characteristics were inferior.

The several advection methods were substituted for the advective term in a simple non-divergent barotropic model. The purpose of this experiment was to test the characteristics of the methods in a realistic, non-linear situation. Operationally produced 500-MB analyses were obtained from FNWC for initial data and for forecast verification.

Twenty-four and forty-eight hour forecasts of the 500-MB height field were produced using each form of the advective equation on eight consecutive map times beginning at 0000Z 15 January 1968. RMSE statistics were compiled for each of the methods on each of the map times. Machine plotted contour maps of all forecasts were generated for the map times 15/1200Z, 17/0000Z, and 18/1200Z. Error charts were also plotted.

Analysis of the RMSE statistics indicated that the relative skill of the methods was inversely proportional to the complexity of the method employed. Furthermore, all experimental methods except the fourth-order conservation form had lower RMSE than did the FNWC forecasts.

Subjective analysis of the prognoses and error charts indicated that the inverse relationship was principally due to a tendency of the high-order equations to deepen existing low pressure centers excessively.

The poor performances of the FNWC progs was attributed to persistent errors in the western Pacific and eastern Asia. The cause of the FNWC errors is unknown.

Detailed analysis of the 15/1200Z map time indicated that the fourth-order methods resulted in more rapid movement of troughs in strong gradient areas than occurred when lower order forms were used. Rapidly moving and deepening low centers were also handled better by the high-order methods, particularly the conservation method. Weakening low centers and static situations were generally handled better by the low-order methods.

FNWC progs gave the best overall trough movement, primarily because of more rapid movement of the southerly portions. FNWC progs were at least equal to the lower order experimental methods when forecasting for weakening cyclones.

Crowley's equations were shown to be stable when subjected to the non-linear conditions of typical weather charts. The theoretical phase and amplitude characteristics appeared to remain valid under these conditions.

No definitive conclusions concerning the relative skill of a barotropic model employing the high-order advective equations could be made. A large number of trials under widely varying initial conditions would be necessary. Such further testing appears to be warranted and desirable in view of the favorable results of the limited experiments conducted thus far.

BIBLIOGRAPHY

1. Crowley, W. P. "Numerical Advection Experiments." Monthly Weather Review, XCVI (January, 1968), 1 - 11.

2. Haltiner, George J. "Numerical Weather Prediction." Unpublished notes, Naval Postgraduate School, 1968.

3. Leith, C. E. "Numerical Simulation of the Earth's Atmosphere," Methods in Computational Physics, Vol. IV. Academic Press, 1965.

4. Lewit, Howard L. "The Experimental Modification of a Barotropic Numerical Prediction Model." Unpublished Master's Thesis, Naval Postgraduate School, 1967.

5. Thompson, Phillip D. Numerical Weather Analysis and Prediction. MacMillan Company, 1961.

INITIAL DISTRIBUTION LIST

		No. Copies
1.	Defense Documentation Center Cameron Station Alexandria, Virginia 22314	20
2.	Library Naval Postgraduate School Monterey, California 93940	2
3.	Professor G. J. Haltiner Department of Meteorology Naval Postgraduate School Monterey, California 93940	1
4.	CDR. Dean R. Morford, USN 2nd Weather Squadron Global Weather Central Offutt Air Force Base, Nebraska 68113	1
5.	Naval Weather Service Command Washington Navy Yard Washington, D. C. 20390	1
6.	Officer in Charge Navy Weather Research Facility Naval Air Station, Building R-48 Norfolk, Virginia 23511	1
7.	Commanding Officer U. S. Fleet Weather Central COMNAVMARIANAS, Box 12 FPO San Francisco, California 96630	1
8.	Commanding Officer U. S. Fleet Weather Facility Box 72 FPO New York, New York 09510	1
9.	Commanding Officer Fleet Numerical Weather Central Naval Postgraduate School Monterey, California 93940	2
10.	Commanding Officer U. S. Fleet Weather Central Box 110 FPO San Francisco, California 96610	1

11.	Commanding Officer U. S. Fleet Weather Central Box 31 FPO New York, New York 09540	1
12.	Commanding Officer Fleet Weather Facility Navy Department Washington, D. C. 20390	1
13.	AFCRL - Research Library L. G. Hanscom Field Attn: Nancy Davis/Stop 29 Bedford, Massachusetts 01730	1
14.	Superintendent Naval Academy Annapolis, Maryland 21402	1
15.	Director, Naval Research Laboratory Attn: Tech. Services Info. Officer Washington, D. C. 20390	1
16.	Naval War College Newport, Rhode Island 02844	1
17.	Department of Meteorology Code 51 Naval Postgraduate School Monterey, California 93940	3
18.	Department of Oceanography Code 58 Naval Postgraduate School Monterey, California 93940	1
19.	American Meteorology Society 45 Beacon Street Boston, Massachusetts 02128	1
20.	Bureau of Meteorology Attn: Library Box 1289 K, G. P. O. Melbourne Vic. 3001 AUSTRALIA	1
21.	Program Director for Meteorology National Science Foundation Washington, D. C. 20550	1
22.	Office of Naval Research Department of the Navy Washington, D. C. 20360	1

23.	Commander, Air Weather Service Military Airlift Command U. S. Air Force Scott Air Force Base, Illinois 62226	2
24.	Headquarters 2nd Weather Wing (MAC) United States Air Force APO New York, New York 09611	1
25.	Atmospheric Sciences Library Environmental Science Service Administration Silver Spring, Maryland 20910	1
26.	Director, Maury Center for Ocean Sciences Naval Research Laboratory Washington, D. C. 20390	1

UNCLASSIFIED

Security Classification

DOCUMENT CONTROL DATA - R & D

(Security classification of title, body of abstract and indexing annotation must be entered when the overall report is classified)

. ORIGINATING ACTIVITY *(Corporate author)* Naval Postgraduate School Monterey, California 93940	2a. REPORT SECURITY CLASSIFICATION UNCLASSIFIED 2b. GROUP

. REPORT TITLE

Numerical Experiments With High-Order Advective Equations

. DESCRIPTIVE NOTES *(Type of report and inclusive dates)*

Master's Thesis

. AUTHOR(S) *(First name, middle initial, last name)*

Dean R. Morford, Commander, USN

. REPORT DATE December 1968	7a. TOTAL NO. OF PAGES 60	7b. NO. OF REFS 5
8a. CONTRACT OR GRANT NO. b. PROJECT NO. c. d.	9a. ORIGINATOR'S REPORT NUMBER(S) 9b. OTHER REPORT NO(S) *(Any other numbers that may be assigned this report)*	

10. DISTRIBUTION STATEMENT

Distribution of this document is unlimited.

11. SUPPLEMENTARY NOTES	12. SPONSORING MILITARY ACTIVITY Naval Postgraduate School Monterey, California 93940

13. ABSTRACT

Second-order and fourth-order two-dimensional advective equations developed by W. P. Crowley were examined to determine their applicability to atmospheric models.

One second-order and two fourth-order forms were evaluated from their performances on a simple pattern advected by a linear, divergent velocity field. The same equations were substituted for the advection term of a simple barotropic forecast model to determine their performances on more general non-linear conditions.

All forms of the equations remained stable in time and demonstrated the phase and amplitude characteristics predicted by Crowley. The fourth-order "advection" form gave best results.

When substituted in the barotropic model, the fourth-order forms lead to improved trough and low-center movements, but RMSE was slightly larger than that resulting from second-order forms. The better RMSE of the lower order forms apparently resulted from their diffusive characteristics.

DD FORM 1 NOV 65 1473 (PAGE 1)

S/N 0101-807-6811

UNCLASSIFIED

Security Classification

A-31408

14. KEY WORDS	LINK A		LINK B		LINK C	
	ROLE	WT	ROLE	WT	ROLE	WT
Advection						
High-order equations						
Jacobian						
Numerical weather prediction						